

FILTER-PRESS DIFFERENTIATION: A NEWLY-RECOGNIZED FRACTIONATION MECHANISM FOR SILICATE INCLUSIONS IN SOMBRERETE AND POSSIBLY IN OTHER IRON METEORITES.

A. Ruzicka and M. Hutson, Cascadia Meteorite Laboratory, Department of Geology, Portland State University, 1721 SW Broadway, Portland, OR 97207-0751, email: ruzickaa@pdx.edu.

Introduction: Sombrorete is an ungrouped silicated iron that we have been studying using petrographic, SEM, microprobe, and SIMS techniques [1,2]. Our data suggest that a novel crystal/liquid fractionation mechanism, which we call “filter-press differentiation”, was responsible for producing bulk-chemical heterogeneity for inclusions in Sombrorete. In this mechanism, the metal host acts as a “filter” to separate liquidus crystals from residual melt in inclusions, allowing only the latter to pass and enabling differentiation to occur. Dynamical forces act as a “press” to allow flow to occur between inclusions.

Inclusion mineralogy and texture: Sombrorete contains several % silicate inclusions located mainly at metal grain boundaries [3]. The silicate inclusions are typically ~2-4 mm across in exposed dimensions, and most are roughly ~5 mm apart from their nearest neighbor. They show clear evidence (e.g., the presence of abundant glass, fine grain size, and skeletal crystal morphologies) of having formed by relatively rapid igneous crystallization [1,3]. Si-rich glass is the predominant phase in most inclusions. Euhedral, typically 6-sided Cl-apatite (*apat*) and elongate orthopyroxene (*opx*) ($\text{Fs}_{27-35}\text{Wo}_{1-4}$) crystals (mainly ~20-100 μm across) are present in most inclusions, but their proportions vary dramatically. Based on their euhedral habit, and their enclosure by other phases, *apat* appears to have been a liquidus and *opx* a near-liquidus phase in the inclusions. They are often aligned in the inclusions, either locally subparallel, somewhat radiating, or in a concentric arrangement. These alignments are probably indicative of fluid flow in the inclusions. Other phases found in the inclusions include plagioclase (An_{70-97}), yagiite, ilmenite, merrillite, chromite, and fine-grained phosphate-rich segregations.

Inclusion composition: Bulk major-element compositions of 20 inclusions in Sombrorete were determined by modal reconstruction (MR) and defocused beam analysis (DBA) techniques. For the MR technique, phase-chemical data obtained with the electron microprobe were combined with modes determined by manual point counting of backscattered electron image mosaics. For the DBA technique, the diameter of the electron microprobe beam was expanded to 20 or 40 μm and multiple analyses across the inclusions were averaged. The two techniques were found to give es-

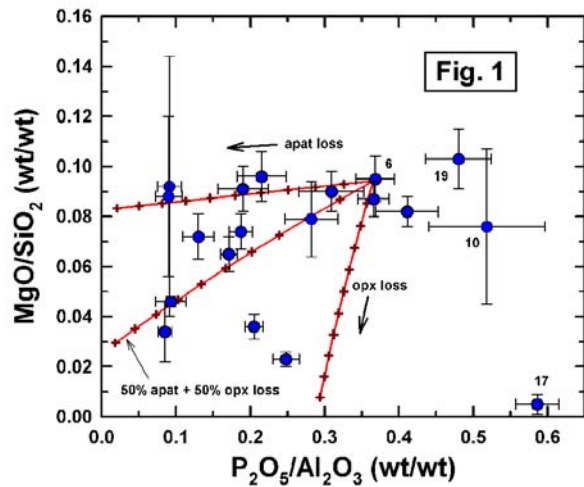
entially identical results, but the MR technique was used as the primary data source for all but the finest-grained inclusions as it usually yielded lower estimated errors.

Observations. The average inclusion composition we determined (~58 wt% SiO_2 , 0.8% TiO_2 , 15% Al_2O_3 , 0.9% Cr_2O_3 , 4% FeO , 0.2% MnO , 4% MgO , 7% CaO , 5% Na_2O , 0.4% K_2O , 4% P_2O_5 , 0.5% Cl) agrees with that determined previously by averaging many focussed microprobe analyses [3] and can be described as a phosphoran, sodic andesite.

The compositions of inclusions in Sombrorete vary significantly. On a total alkali - silica diagram, compositions range mainly from basaltic andesite (~55 wt% SiO_2) to dacite (~65% SiO_2), with a relatively high alkali content (~4-6% $\text{Na}_2\text{O} + \text{K}_2\text{O}$). Three inclusions have compositions that fall into the trachy-basalt and trachy-basaltic andesite fields. Inclusions containing the lowest silica content tend to be the most enriched in *apat*-sited (P_2O_5 , CaO , Cl) and *opx*-sited (MgO , FeO) components. Those containing the highest silica contents are most enriched in Al_2O_3 , both of which are concentrated in glass. This implies that variations in the proportions of glass, *apat*, and *opx* are mainly responsible for the bulk-chemical variations.

Models. Bulk-chemical compositions were modelled assuming that variable amounts of *apat* and *opx* were fractionated from a common, silica-poor precursor, which we equated to one of the larger, silica-poor inclusions in Sombrorete (Som-6). Example results are shown in Fig. 1, which compares observed compositions to model fractionation lines produced by removal of *apat* alone, *opx* alone, or a 50/50 mixture of the two phases. Tick marks on fractionation lines in Fig. 1 show 10% loss increments relative to the starting amounts of *apat* and *opx* present in Som-6 (~10 and 17 vol%, respectively). The data imply that relative to Som-6, most inclusions in Sombrorete can be explained by loss of anywhere from 10-80% Cl-apatite alone or 10-80% loss of a 50/50 mixture of Cl-apatite and orthopyroxene (Fig. 1). Some inclusions cannot be readily explained by this model; these include Som-10, 17, and 19, which have higher phosphate abundances than the assumed Som-6-like precursor. Som-10 and 19 could represent alternative starting compositions, although they are smaller inclusions with less well-determined compositions. On balance, the composi-

tions of most inclusions, including all major and minor elements, can be fit rather well by this model.



Glass composition: Glass compositions in the inclusions vary somewhat, with variation in Ca content (from ~0.3 to 2.2 wt%) being one of the most notable features. Glass chemistry provides additional evidence for the operation of a filter-press mechanism involving phosphate segregation between inclusions.

Fig. 2 shows the average glass Ca content in different inclusions vs. bulk inclusion P_2O_5 and SiO_2 contents. Crystallization of *apat* would result in removal of Ca from the residual melt. If this removal occurred *in situ*, one would expect a negative correlation between glass Ca content and bulk P_2O_5 content, as the latter is principally sited in phosphate. However, the data show instead a crude positive correlation between glass Ca content and bulk P_2O_5 content (Fig. 2a). A positive trend is consistent with the filter-press model, because it implies that the most fractionated glasses are those that contain the least amount of phosphate currently. This phosphate would have been sequestered, even as the melt (glass) recorded its crystallization and removal. Similarly, a crude negative correlation is observed between glass Ca content and bulk inclusion SiO_2 content (Fig. 2b). This is opposite to the trend predicted for *in situ* crystallization, and consistent with the trend predicted for the filter-press model. Thus, inclusion differentiation evidently proceeded from low to high bulk silica content, high to low bulk P_2O_5 , and high to low glass Ca content (Fig. 2).

Summary: Chemical heterogeneity for inclusions in Sombroerete is best explained by a model in which the metal host acted as a “filter” to prevent crystals of liquidus phases (*apat* and *opx*) from passing, but allowing silicate melt to pass. This implies that silicate

melt was flowing through the meteorite, which is consistent with textural evidence for flow processes occurring inside inclusions. Flow was able to occur despite relatively rapid cooling. The metal host itself was probably at least partly liquefied, so as to allow silicate melt to move through and re-arrange within the host, resulting in no significant void space. The model implies that in Sombroerete, a single precursor liquid composition, similar to a phosphoran alkali basaltic andesite, evolved locally to dacite within the confines of the metal. A similar type of filter-press model may have operated in other silicated iron meteorites (e.g., IIE and IAB). Like Sombroerete, other silicated irons often show wide ranges in bulk inclusion compositions with only modest changes in phase compositions [e.g., 4-6], features that can be explained by filter-press differentiation.

References: [1] Ruzicka A. and Hutson M. (2003) *MAPS* 38, A129. [2] Ruzicka A., Hutson M., and Floss C. (2005) ms in prep. [3] Prinz M. et al. (1982) *LPS XIII*, 634-635. [4] Bunch T.E., Keil K., and Olsen E. (1970) *CMP* 25, 297-340. [5] Ruzicka A. et al. (1999) *GCA* 63, 2123-2143. [6] Benedix G.K. (2000) *MAPS* 35, 1127-1141.

